JOURNAL OF SOLID STATE CHEMISTRY 4, 391–399 (1972)

Effect of Pressures to 50 kbar on the Magnetic Behavior of MnP*

M. D. BANUS†

Lincoln Laboratory, Massachusetts Institute of Technology,
Lexington, Massachusetts 02173

Received August 23, 1971

The change with pressure in the magnetic-ordering temperature ($T_c = 291.5$°K at 1 atm) of polycrystalline and single-crystal MnP has been investigated by monitoring the change with temperature in initial permeability of bifilar-wound toroids and a "picture frame" subject to hydrostatic pressures to 30 kbar and quasihydrostatic pressures to 50 kbar. From 1 atm to 20 kbar the T_c for MnP decreases linearly: $\Delta T_c/\Delta P = -1.85$°K/kbar. Between 20 and 30 kbar the slope $\Delta T_c/\Delta P$ changes continuously to −2.5°K/kbar. Above 30 kbar the shape of the initial susceptibility vs temperature curve is altered to that characteristic of antiferromagnetic ordering, and $\Delta T_c/\Delta P$ appears to change sign. A ferromagnetic–antiferromagnetic transition may reflect either an increase in the metamagnetic transition temperature T_t with pressure ($T_t = 50$°K at 1 atm) or band broadening that approaches the limiting width that can support spontaneous magnetism. Although T_t was not specifically monitored, failure to find $T_t > 57$°K at 9 kbar argues against the first alternative. In addition, a sharp peak in the initial permeability curves about 7–9°K below T_c was shown to be due to magnetic anisotropy.

The ferromagnetic-ordering temperature (T_c) of orthorhombic MnP has been determined to be 291.5°K by Huber and Ridgley (*1*) using a single-crystal sphere. No change from the $B31$ crystal structure accompanies this magnetic ordering. They also found MnP to exhibit an antiferromagnetic–ferromagnetic transition at 50°K (T_t); below this temperature it is metamagnetic. Hirahara, Suzuki and Matsumura (*2*) used electrical-resistivity measurements of a single crystal to monitor these two transitions as a function of uniaxial pressure. Pressures to ~2 kbar were applied along the *a*, *b*, and *c* crystallographic axes. Pressure applied along the *a* axis caused a decrease in T_c of 35°K/kbar and an increase in T_t of 6.3°K/kbar; along the *b* and *c* axes, it caused a small increase in T_c and a small decrease in T_t. Subsequently, Kamigaichi, Okamoto, Iwata and Tatsumoto (*3*) followed the change of T_c and T_t with hydrostatic pressure on a polycrystalline ingot of MnP, again using small changes in electrical resistance to identify these transitions. Hydrostatic pressure on the polycrystalline mass integrated the pressure effects along the three axes. They found that T_c decreased linearly to 6 kbar with $\Delta T_c/\Delta P = -1.5$°K/kbar, that T_t decreased nonlinearly at about the same rate to 5 kbar. This decrease in T_t does not appear consistent with the uniaxial data, since the single-crystal data showed that the sign of dT_t/dP was always opposite to that of dT_c/dP.

MnAs also has the orthorhombic $B31$ structure just above a ferromagnetic Curie temperature $T_c = 317$°K. However, in MnAs ferromagnetic ordering is accompanied by a first-order phase change to the hexagonal $B8_1$ structure of NiAs. The transition temperature decreases with increasing pressure ($dT_c/dP = -13.8$°K/kbar) to 4.5 kbar (*4*). Above this pressure, the orthorhombic phase is stable to lowest temperatures; a second-order magnetic transition near 240°K, which has $dT_N/dP = 1.4$°K/kbar and $T_N > T_c$, appears to stabilize the $B31$ structure. Although two distinguishable metamagnetic phases are found below T_N, the ferromagnetism induced by an external field has a reduced magnetization and does not accompany a phase change to hexagonal ($B8_1$) symmetry. Above 8 kbar, the two metamagnetic phases are separated by a ferromagnetic phase, and the temperature

---

* This work was sponsored by the Department of the Air Force.

† Present address: B.U. Marine Program, Marine Biology Laboratory, Woods Hole, MA 02543.

range of this ferromagnetic phase increases with pressure, particularly on the high-temperature side, until above 12 kbar a $T_c > T_N$ occurs (*5*). Thus high-pressure ($P > 12$ kbar) MnAs has structural and magnetic properties similar to those found in MnP. It therefore seemed interesting to investigate whether the ferromagnetic phase of MnP could be suppressed by the application of higher hydrostatic pressures and whether the magnetic transition would decrease continuously to zero. Furthermore, Goodenough (*6*) has predicted that at lowest temperatures there should be a transition from ferromagnetism to antiferromagnetism to paramagnetism with increasing bandwidth, and hence with increasing pressure.

The change with pressure in magnetic-ordering temperature of polycrystalline and single-crystal MnP was studied by observing the change with temperature in initial permeability of a bifilar-wound toroid subject to hydrostatic pressures to 30 kbar and quasi-hydrostatic pressures (solid pressure-transmitting medium AgCl) to 50 kbar. From 1 atm to 20 kbar the T_c for MnP decreases linearly, $\Delta T_c/\Delta P = -1.85$°K/kbar. Between 20 and 30 kbar, the slope $\Delta T_c/\Delta P$ changes continuously to -2.5°K/kbar and the shape of the initial susceptibility vs temperature curve is altered. Above 30 kbar the shape of this curve suggests an ordering other than ferromagnetic. In addition, strong magnetic-anisotropy effects were observed.

Experimental

The MnP ingots were prepared by the technique described by Huber and Ridgley (*1*). "Specpure" Mn from Johnson Matthey was distilled under high vacuum at 1150 ± 20°C from a "Morganite" crucible to remove oxides. The bright, freshly distilled Mn was placed in a degassed "Morganite" crucible at the upper end of a 30 cm × 2.5 cm fused silica tube; and the appropriate amount of red phosphorus (Gallard Schlesinger 6-9's) was placed in a second crucible above the Mn. After degassing and evacuation to $\sim 1 \times 10^{-5}$ torr, the tube was sealed and placed in a vertical two-zone furnace. For the first 20 hours the top was heated to ~680°C while the bottom was kept at ~300°C to convert any white phosphorus to the red modification. Then the top was raised to ~1170°C and the bottom to 380°C and held for 1–2 days.

To grow a single crystal, the top was slowly program-cooled (~2.5°C/hr) to 1000°C, at which temperature the controllers were shut off. In general, the MnP came out as a solid single-crystal ingot, ~1.5–2.5 cm across by ~1 cm high, with a few gas holes in the bottom half. The orientation of the crystals varied over the several preparations. Occasionally there was a polycrystalline zone on top that could be easily trimmed off. In one run, the ingot was coarsely polycrystalline throughout. The X-ray Debye–Scherrer patterns for these crystals showed only the lines of MnP, and the lattice constants calculated from these patterns agreed with published data.

Magnetic measurements were made using an ac method on washer-shaped specimens, which provided the core of a transformer. These specimens were cut either from short rods cast from a mixture of MnP powder dispersed in epoxy cement, from slices of polycrystalline ingot, or from single-crystal ingots. The specimens were coated with teflon or durathane before winding with #44 copper wire, hardcoated with teflon or Formvar. This technique has been described by McWhan and Stevens (*7*). The electronics used were similar to the equipment and circuitry shown in Fig. 2 of that reference. In the present study, the input frequency was 1000 cps, the thermocouple was iron–constantan and the bucking sample was omitted.

For measurements under hydrostatic pressure, the sample was placed in a liquid cell machined from pressed AgCl and pressed in a 1 in. piston-cylinder unit capable of pressures to 30 kbar (Fig. 1). The liquid was a 50–50 by volume mixture of iso-amyl alcohol and pentane. The sample was cooled to about 150°K by blowing liquid N_2 through the cylinder body jacket. It was then heated by blowing heated dry N_2 through the same jacket followed by heated water. At the start of the cooling cycle, all water had to be blown out to prevent clogging the jacket with ice. A typical cool-heat cycle started at 310–320°K, went down to 170–180°K, which is well below T_c, and then returned to the initial temperature. It was not possible to attain temperatures low enough to follow the metamagnetic transition temperature $T_t \approx 50$°K. Plots of relative secondary voltage vs thermocouple output were made by the X–Y recorder during the entire cycle, the zero being shifted a little at lowest temperatures in order to separate the two traces.

Measurements were made to 50 kbar using a 0.5 in. girdle-die of the type described by Stromberg and Stevens (*8*). The specimen configuration was similar to the one shown in Fig. 1 of Ref. (*7*) (with the axial calibration sample omitted). The die, pistons, and backing blocks were placed inside a polyurethane-foam-insulated stainless-steel tank. This assembly and 1/2 in. lamitex spacers to increase

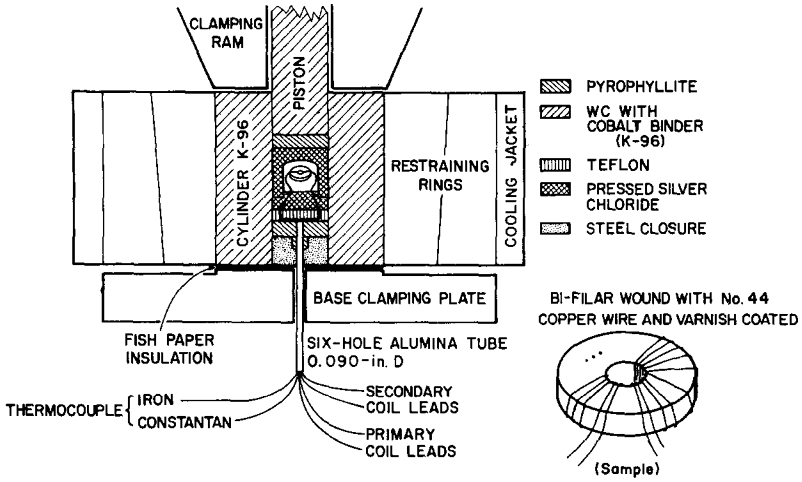

FIG. 1. High-pressure liquid cell in 1 in. piston-cylinder pressure unit. End loading on the carbide cylinder was provided by 400 tons applied between the clamping ram and base clamping plate mounted in a 600-ton platten press. An auxiliary pressure system supplied up to 200 tons loading to the piston. The six wires were sealed to the high-pressure end of the alumina tube by epoxy cement.

the thermal insulation were mounted between the plattens of a 300 ton press. Liquid N_2 was slowly added to the tank to cool the die and sample. Air, heated to ~200°C, was blown around the die to heat it. The electronic circuit was too sensitive to any ac currents to use electrical heating. Extraneous electrical signals made the signal-to-noise ratio a major problem with this unit. Careful shielding and grounding could only partially change this ratio, which was particularly low at high pressures where maximum amplification of the secondary-voltage signal was required.

For all pressure runs, the desired pressure, determined from previous equipment calibration, was set with the system at room temperature and was maintained during the cool-heat cycles by sensitive load-cell and wheatstone-bridge circuits. Pressure changes were made only when the system was close to room temperature. It is possible that the actual pressures on the samples at low temperatures (150–170°K) are different from the calibrated pressures at 300°K due to changes in the relative compressibilities and thermal expansions of the various materials around the sample. All cooling–heating cycles were made at increasing pressure points, since calibration experiments had shown this to be most reliable. Two or more cycles were made at each pressure on each sample in order to check both the shape of the curves and the transition temperatures determined from them. In general, several rings of each type were run under similar conditions to be sure each ingot was self-consistent.

Results

Curves of secondary voltage vs thermocouple output voltage clearly show a change at T_c (Figs. 3–7). Up to 20–25 kbar the data from the single-crystal rings and from the powdered MnP-epoxy castings showed excellent agreement, both in the hydrostatic system and in the girdle-die. These data are listed in Table I. The values for the individual pressures are the average of all the runs at that pressure. The indicated temperature range is between values from the cooling and heating parts of the cycle. In the girdle-die, there was substantially more hysteresis, so that the cooling value of T_c was as much as 8° below the heating value. This may have been caused by the poorer control of the heating and cooling rates in this equipment.

Selecting the point of the curve to take as T_c presented some problem, since the slopes of the curves varied between crystal orientations and between powder-epoxy and crystal rings, as will be discussed later. In addition, the shapes of the curves changed substantially with increasing pressure in some cases. For the powder-epoxy samples, T_c was taken as the temperature of the midpoint of the change in secondary voltage. For the single-crystal rings, where there was a sharp peak, the temperature of this peak was taken. Both of these methods gave good agreement with the previously reported T_c for MnP at 1 atm (*1*).

The change in T_c with pressure is shown in Fig. 2. It is linear from 1 atm to ~20 kbar with $\Delta T_c/\Delta P = -1.85$°K/kbar. At higher pressures the slope appears

TABLE I

TEMPERATURE (°K) OF CRITICAL POINTS OBSERVED IN INITIAL PERMEABILITY CURVES

Pressure	Crystal #10-736 (liquid cell)	Crystal #10-799 (liquid cell)		Powder in epoxy (liquid cell)		Powder in epoxy (girdle)	
	Temp. of peak	Temperature of:		Temperature of:		Temperature of:	
		First peak	Second peak	Midpoint of voltage change	New peak	Midpoint of voltage change	New peak
1 atm	291 ± 1	291 ± 1	283 ± 1	293 ± 2			
2 kbar	288 ± 1	289 ± 1	280 ± 1	291 ± 5		285 ± 4	
5 kbar	283 ± 1	282 ± 1	273 ± 1	283 ± 0.5			
10 kbar	273 ± 1.5	273 ± 2	265 ± 2	274 ± 1		272 ± 3	
15 kbar	264 ± 1.5	265 ± 1.5	257 ± 1.5				
20 kbar	254 ± 1	254 ± 1	247 ± 1	248 ± 1		247 ± 4	
25 kbar	239 ± 1	242 ± 0.5	235 ± 0.5	242 ± 1	222 ± 1	239 ± 2	
30 kbar				233 ± 1	221 ± 1	228 ± 3	210 ± 1
35 kbar						223 ± 2	210 ± 1
40 kbar						221 ± 2	208 ± 1
50 kbar						235 ± 7	225 ± 10

to increase. However, this may be due to the changing shape of the curves as shown in Fig. 3. Above 20 kbar, the secondary-voltage vs temperature curves assume the characteristic shape of a transition to antiferromagnetic ordering, so that the peaks in the curves at 25, 30, 35 and 50 kbar may be at the temperatures of a T_N for a new magnetic phase. Therefore, taking the midpoint of the change in secondary voltage may be meaningless at 25 and 30 kbar, and it certainly is at 35 kbar and higher pressures. In this figure, the curves at 30 kbar and below were made in the hydrostatic system while those at 35 and 50 kbar were made in the girdle-die. However, the curves at the lower pressures in the girdle-die are very similar in shape to those made in the liquid cell, the major difference being a larger hysteresis and a smaller secondary voltage for the former.

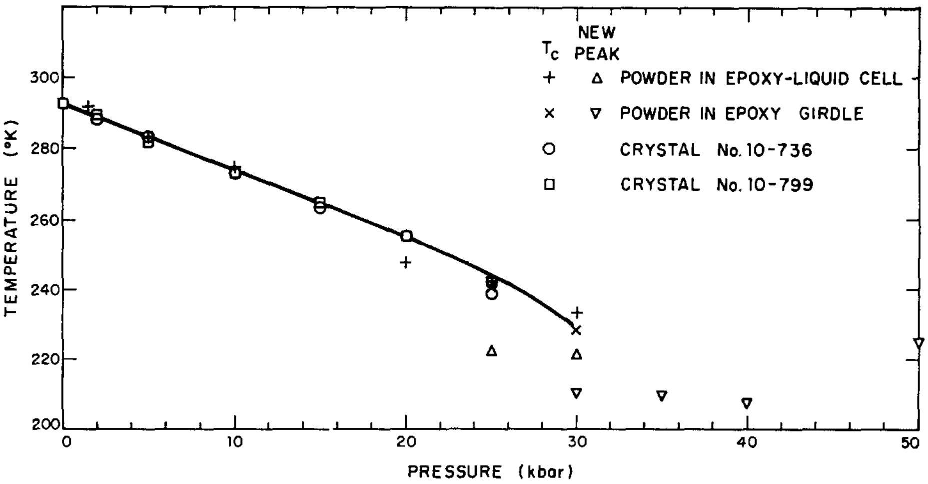

FIG. 2. Effect of pressure on the Curie temperature (T_c) of MnP. The slope, dT_c/dP, is −1.85°K/kbar between 1 atm and 20 kbar.

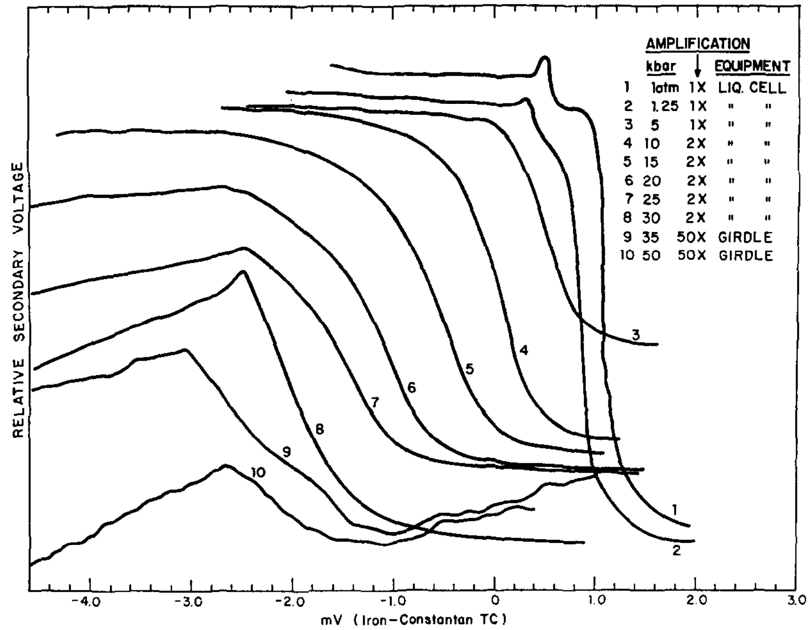

FIG. 3. Relative secondary voltage vs thermocouple output in mV for MnP powder dispersed in epoxy cement. There was 50–75 wt% MnP in the cast samples. The washer-shaped specimens were bifilar wound over ~85% of their circumference. Curves #9 and #10 emphasize the greater amplification required for the samples in the girdle pressure cell and the resulting increase in noise. (Curves for Figs. 3–7 were traced directly from the *X–Y* plots made during the cooling portion of the cool–heat cycles.)

In Fig. 2 are plotted the temperatures of the peaks of the secondary voltage vs temperature curves for the high-pressure ($P \geqslant 25$ kbar) runs. These peaks appear about 10° higher in the hydrostatic equipment than in the girdle-die unit, which gives an apparent decrease between 30 and 35 kbar in the temperature for the peak. However, if the data for just the girdle-die is considered (Table I), there is little change for this peak between 30 and 40 kbar, but there is a definite increase in temperature for this peak at 50 kbar. This suggests that between 25 and 35 kbar the magnetic phase below the magnetic-ordering temperature changes from ferromagnetic to antiferromagnetic. If the transitional phase is metamagnetic, as predicted by Goodenough (*6*), then the transitional pressure would be poorly defined. Although the system is hydrostatic at 30 kbar and room temperature, at 220°K it is probable that the iso-amyl alcohol–pentane mixture is also a solid. This might contribute to a smearing of the transitional pressure. Nevertheless, at 25 kbar the single-crystal torroids were not damaged after cooling to 160°K, so there were no appreciable stress inhomogeneities under these conditions.

At 1 atm the curves for the secondary voltage vs thermocouple output for several powder-epoxy samples exhibited an anomalous peak—see Fig. 3 for a typical example—which is not characteristic of a simple ferromagnetic ordering. Since MnP has an exceptionally large magnetic anisotropy, this anomaly was studied in two single-crystal specimens, cut in the form of washers, and in one single-crystal "picture frame" oriented with respect to the crystal axes. Both a powder-epoxy ring with carefully positioned winding and rings from polycrystalline ingots were also studied at ~1 atm. The influence of winding position on single-crystal and polycrystal ring samples was carefully investigated to demonstrate the sensitivity of the shape of the permeability curves to the position of the windings relative to the crystallographic axes.

Washers cut from the first single-crystal ingot, #10-736, whose axis had no close relationship to any crystallographic direction, gave the curves shown in Fig. 4. These curves have very sharp peaks and sharp changes in secondary voltage, so that the peak temperature is essentially the same as the temperature for the midpoint of the voltage change. The valley in the curve below the peak gradually flattens out with pressure, so that at 25 kbar it is nearly gone and the shape is approximately that for a typical ferromagnetic transition. This is in contrast

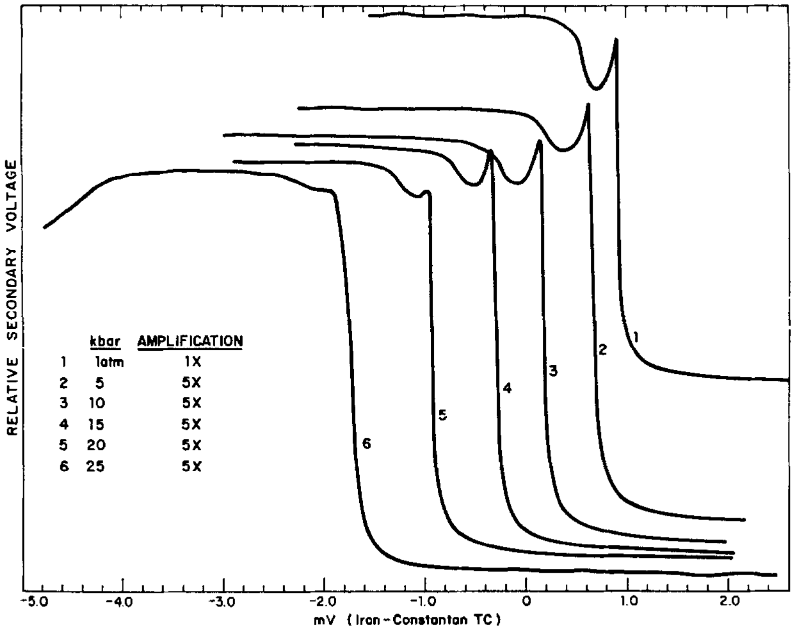

FIG. 4. Relative secondary voltage vs thermocouple output for rings of crystal #10-736. The axis of these washers had no close relationship to the crystallographic axes.

to the results of Fig. 3 for the powder-epoxy ring, which show a new peak starting to appear at this pressure.

A washer was cut from a second crystal, #10-799, with the axis ~10° off the ⟨001⟩ direction. Thus the ⟨100⟩ and ⟨010⟩ directions were in the plane of the ring and covered by windings. Three typical curves obtained on this sample are shown in Fig. 5. The first sharp peak coincides with the T_c at 1 atm as well as the peaks for crystal #10-736 at pressure. The second, much taller, peak is 8–9° below the first at lower pressures and 7° below at 20 and 25 kbar. The temperature of this peak coincides with the small peak observed at 1 atm and 1.25 kbar with the powder-epoxy samples. Pressure suppresses this peak in relation to the first peak. At 25 kbar, the overall shape of the curve may be considered similar to that for the powder-epoxy rings at 30 kbar. Thus the change in shape of the latter between 20 and 35 kbar may be due to an orientation effect enhanced by pressure rather than to a change to antiferromagnetic ordering. However, the change to a positive $\Delta T_c/\Delta P$ above 35 kbar is more likely to be caused by a new magnetic phase.

To find out whether the ⟨010⟩ or ⟨100⟩ direction is responsible for the second peak, a square "picture-frame" was cut from a slice of crystal #10-752 with the face of the slice in the (001) plane. This specimen was wound so that either only the ⟨010⟩ direction or the ⟨100⟩ direction was used. The curves (Fig. 6) clearly show that the ⟨010⟩ direction is responsible for the second peak. Therefore, the double peak observed for crystal #10-799 appears to indicate that the ⟨010⟩ direction was covered by most of the winding.

However, the ingot shape did not make it possible to cut a specimen so that the ⟨001⟩ direction could be included or excluded from the windings. The first peak, which shows up in all single-crystal samples and even in a polycrystalline sample (#TS-2, Fig. 6), may be at least partially due to the inclusion of the ⟨001⟩ direction in the windings. However, the *c* axis is the "easy" magnetic direction (*1*).

Some preferred orientation of the MnP powder particles must occur during dispersion and casting in epoxy cement at room temperature, since some rings show one or more of the peaks observed with the single-crystal rings. This is further demonstrated by the secondary voltage vs thermocouple voltage curves shown in Fig. 7. Ring A, which was wound around its entire circumference, gave a curve with the shape expected for a randomly oriented powder going through ferromagnetic ordering, except for a small peak about 10°K below the T_c. Therefore, the MnP particles had little preferred orientation. However, a second ring, B, was indexed so that it could be wound around a definite part of its circumference. With the first position of the windings, it

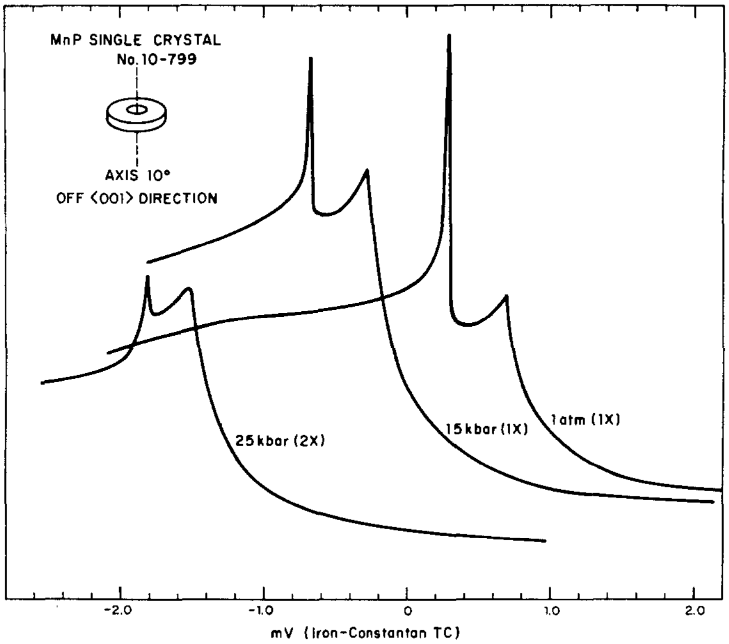

FIG. 5. Three typical curves of relative secondary voltage vs thermocouple output for rings cut from crystal #10-799. The face of the washer was close to the (001) plane so that the ⟨100⟩ and ⟨010⟩ directions are covered by the windings and effected by the magnetic field.

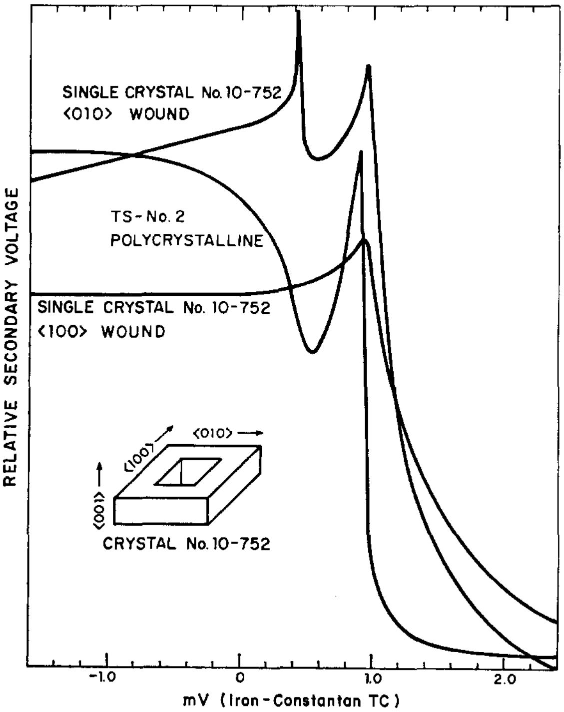

FIG. 6. The effect of winding a specific crystallographic axis on the shape of the relative secondary voltage vs temperature curve. The polycrystalline sample has a curve very similar to the one from crystal #10-736 (Fig. 4).

had two peaks of about the same height. When ring B was rewound, moving the wound portion 45° along the circumference, both peaks were sharper and the second peak became the taller, so that the curve is similar to the one for the ⟨010⟩ direction. Therefore, the MnP particles had apparently oriented themselves so that this direction predominated.

Discussion

The decrease in T_c with pressure, $\Delta T_c/\Delta P = -1.85$°K/kbar, between 1 atm and 20 kbar is in reasonable agreement with that reported by Kamigaichi et al. (*3*), who monitored a small change in slope at T_c of electrical resistivity vs temperature. Similar resistivity measurements were repeated in this study; they gave a greater spread between runs and less confidence in the value of T_c for a given run than did the magnetic measurements reported here. Thus the difference in the $\Delta T_c/\Delta P$ value reported here and by Kamigaichi et al. would seem to be due to the difference in experimental technique as well as to the much greater pressure range of this study.

The unique shapes of the initial permeability vs temperature curves initially noted at low pressures on MnP powder-epoxy cast rings, is clearly due to the large magnetic anisotropy of this compound.

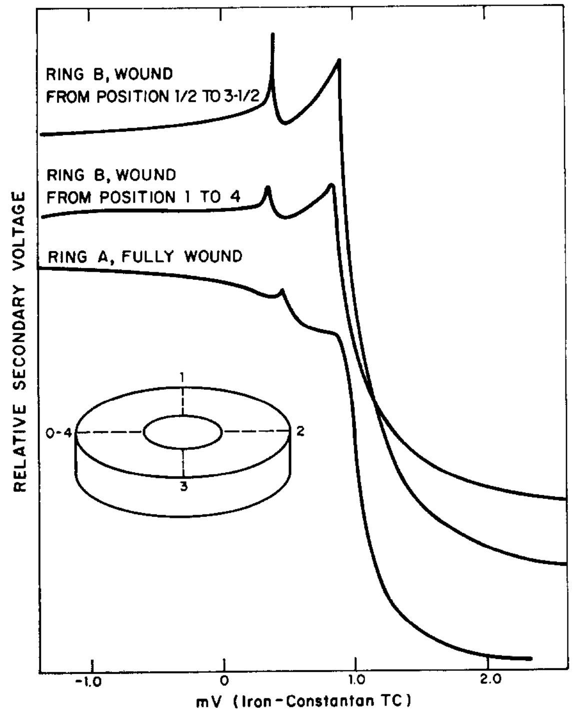

FIG. 7. Evidence for preferred orientation in rings cut from MnP powder cast in epoxy cement. Since MnP is ferromagnetic at room temperature, curing the epoxy slowly prevents heating the MnP above R.T. and therefore permits magnetic interactions between the MnP particles resulting in preferred orientation.

Also, the fact that the shapes of these curves could be influenced by positioning of the wire windings indicates the existence of preferred orientation in these castings. Measurements of initial permeability on single-crystal MnP samples are able to manifest the crystalline anisotropy because only very low magnetic fields (~1 Oe) are generated in the experiment. Using the axes convention $a > b > c$, Huber and Ridgley (*1*) reported a magnetically "hard" *a* axis, an "easy" *c* axis, and an intermediate *b* axis. The curve in Fig. 1 for winding along only the ⟨100⟩ direction, which creates a field along the hard direction, shows no anomalous structure. However, a pronounced anomalous peak 9°K below T_c appears if the winding, and hence external field, is along the intermediate ⟨010⟩ direction. Although no explanation of this anomaly has been established, it is not unreasonable to suspect a competition between shape and crystalline anisotropy. Shape anisotropy would vary with a smaller power of the magnetization and would therefore be competitive only in the vicinity of T_c.

The abrupt change in dT_c/dP and in the character of the initial-permeability curves for pressures $P > 25$ kbar are significant and strongly suggest a ferromagnetic to antiferromagnetic transition in the pressure interval $25 < P < 35$ kbar. Two possible explanations for such a transition are available: either the low-temperature, metamagnetic phase, which appears below $T_t \approx 50$°K in MnP at atmospheric pressure, is stabilized by pressure relative to the ferromagnetic phase ($dT_t/dP > 0$) or pressure broadens the *d* bands sufficiently that the ferromagnetic-to-antiferromagnetic transition predicted by Goodenough (*6*) is induced. Roger and Fruchart (*9*) have observed a $dT_c/dx < 0$ and a $dT_t/dx > 0$ in the system $Mn_{1-x}Fe_xP$, a $T_t = T_c$ occurring at $x \approx 0.12$, and the cell volume decreases with *x*. Although this suggests an analogous situation might occur in MnP under pressure, the two situations cannot be properly compared. Substitution of FeP increases the electron/atom ratio whereas application of pressure does not. Furthermore, Kamigaichi et al. (*3*) were able to monitor T_t vs *P* as well as T_c vs *P*, and they reported a *decrease* in T_t of 6°K at 5 kbar. Therefore dT_t/dP would have to reverse its spin between 5 and 10 kbar and then increase to at least 7°K/kbar for the low-temperature metamagnetic phase of MnP to be the only stable magnetic phase at 35 kbar. Since Menyuk (*10*), using the equipment described in Ref. (*5*), failed to observe any transition to the antiferromagnetic phase at 9 kbar down to 57°K, such a change in slope of this magnetic-phase boundary is unlikely. These data seem to eliminate the first plausible explanation of the apparent ferromagnetic-to-antiferromagnetic phase change in MnP in the pressure interval $25 < P < 35$ kbar.

Goodenough (*6*) has argued that at lowest temperatures a compound having a partially filled, narrow band may undergo a transformation, with increasing bandwidth, from spontaneous ferromagnetism to a ferromagnetic-spiral to an antiferromagnetic spin-density wave to Pauli paramagnetism. In MnAs and MnP, the orthorhombic *B*31 structure is associated with low-spin manganese ions (*5*, *11*), and the spontaneous ferromagnetism appears to be itinerant-electron, rather than localized-electron, ferromagnetism. Furthermore, the fact that FeP has an antiferromagnetic spin-density wave suggests that transformation from a ferromagnetic to an antiferromagnetic state may be induced in MnP with a relatively small increase in bandwidth. Since the widths of the occupied 3*d* bands of MnP are sensitive to the Mn–Mn interactions (not the Mn–P–Mn interactions), the relevant bandwidths may increase sensitively with hydrostatic pressure. Therefore a ferromagnetic-to-antiferromagnetic transition due to increasing bandwidth, as discussed by Goodenough (*12*) for the system $CoS_{2-x}Se_x$, seems to be a viable explanation of the changes in dT_c/dP and in the shapes of the initial-permeability curves for MnP that are shown in Figs. 2 and 3 for the pressure range $25 < P < 35$ kbar.

Acknowledgments

The author thanks J. B. Goodenough for suggesting this problem and the two possible interpretations of the highest-pressure data, N. Menyuk for many helpful discussions about the magnetic measurements and their interpretation, and T. E. Stack for assistance in carrying out the crystal-growth and pressure experiments.

References

1. E. E. Huber, Jr. and D. H. Ridgley, *Phys. Rev.* **135A**, 1033 (1964).

2. E. Hirahara, T. Suzuki, and Y. Matsumura, *J. Appl. Phys.* **39**, 713 (1968).

3. T. Kamigaichi, T. Okamoto, N. Iwata, and E. Tatsumoto, *J. Phys. Soc. Japan* **24**, 649 (1968).

4. J. B. Goodenough and J. A. Kafalas, *Phys. Rev.* **157**, 389 (1967).

5. N. Menyuk, J. A. Kafalas, K. Dwight, and J. B. Goodenough, *J. Appl. Phys.* **40**, 1324 (1969).

6. J. B. Goodenough, "Progress in Solid State Chemistry" (H. Reiss, Ed.), Chapter 4, Pergamon Press, Oxford, 1971.

7. D. B. McWhan and A. L. Stevens, *Phys. Rev.* **139**, A682 (1965).

8. H. D. Stromberg and D. R. Stevens, *J. Phys. Chem. Solids* **25**, 1015 (1964).

9. A. Roger and R. Fruchart, *Compt. Rend.* **264**, 508 (1967).

10. N. Menyuk, private communication.

11. J. B. Goodenough, D. H. Ridgley, and W. A. Newman, "Proceedings Int. Conf. Magnetism, Nottingham, 1964", p. 542, The Institute of Physics and The Physical Society of London, 1965.

12. J. B. Goodenough, *J. Solid State Chem.* **3**, 26 (1971).